

Biodegradation of cellulose in electric field-assisted biodegradation process: role of low-voltage electric field

Bo Zhang^a, Zhangxing Xu^b, De Qing Yang Zong^b, Defang Ma^{b,*}, Yan Wang^{b,c,*}

^aTechnology Center, China Tobacco Hunan Industrial Co., Ltd., Changsha 410007, China, email: 1079705258@qq.com

^bShandong Key Laboratory of Water Pollution Control and Resource Reuse, School of Environmental Science and Engineering, Shandong University, Qingdao 266237, China, Tel.: +86 13075359293; emails: defangma@sdu.edu.cn (D. Ma), 760359671@qq.com (Z. Xu), 2320598255@qq.com (D.Q.Y. Zong)

^cThe Key Lab of Eco-restoration of Regional Contaminated Environment, Shenyang University, Shenyang, China, Tel.: +86 531 88361812; Fax: +86 531 88364513; email: wangyan824@sdu.edu.cn (Y. Wang)

Received 6 February 2023; Accepted 12 May 2023

ABSTRACT

The decomposition of cellulose plays a critical role in composting agricultural wastes. In this study, the electric field-assisted biodegradation (EAB) process was employed to degrade cellulose. To assess the effect of the electric field, we examined the physicochemical properties of cellulose and the physiological state of microorganisms. The results showed that the degradation rate of cellulose in EAB was significantly higher than that in the biodegradation process alone. Specifically, the degradation rate of cellulose increased with increasing electric field intensity, with a 2.57-fold increase observed after 24 h when the electric field intensity was 2 V/cm. Compared to the biodegradation process, EAB resulted in a greater reduction in cellulose crystallinity. The cellulose surface became rougher and more wrinkled in EAB, which facilitated bacterial adherence. Furthermore, when an external electric field with an intensity of 2 V/cm was applied, the microbial ATP activity showed a 6-fold increase compared to that without any external electric field. This implies that the microbial metabolic activity could be enhanced by utilizing a low voltage external electric field. Additionally, the electric field was observed to increase the permeability of the bacterial cell membrane by 5%–27%, which can facilitate the transportation of substances into the cells.

Keywords: Cellulose; Electric field; Biodegradation; Metabolic activity

1. Introduction

As one of the largest agricultural countries, China has witnessed a steady increase in the generation of agricultural waste, which includes crop straws, sugarcane bagasse waste, and vegetable waste [1]. The current predominant methods of disposing of agricultural waste in China involve incineration, landfilling, and composting. Composting, viewed as a sustainable approach, leverages indigenous microbes and enzymes to recycle agricultural waste [2,3]. During composting, agricultural waste converts into stable humus substances,

which are transformed into soil that serves as a natural fertilizer [4]. The readily available fractions of agricultural wastes can be immediately utilized by composting microbes; however, it is difficult to degrade cellulose in agricultural wastes, which would decrease the efficiencies of composting and reduce the final compost quality [5]. Given this, it is of significant importance to study an effective method for enhancing the degradation efficiencies of cellulose.

Composting is a complex biological redox process in which electrons are generated and transferred to intracellular electron acceptors and then to the respiratory chain

* Corresponding authors.

[6]. Strengthening electron transfer in the biological oxidation-reduction process can accelerate the degradation of organic matters [7]. Conductive mediators, such as bio-char [8], activated carbon, and carbon nanotubes have been proven to significantly enhance the direct interspecies electron transfer in composting or anaerobic digestion process [8–10]. Besides conductive mediators, applied electric field can promote electron transfer more directly. Under the influence of an electric field, the electrons are forced to flow, improving the efficiency of the composting process [11]. It was demonstrated that the electric field-assisted biodegradation (EAB) process exhibits a higher degradation rate compared the conventional biodegradation process [7]. Additionally, EAB has been found to generate a diverse range of simple organic components such as polyphenols, carboxyl, polysaccharide and reducing sugars, which can serve as precursors to form humic substances [12].

Cellulose is a linear homopolysaccharide composed of glucose linked by β -1,4 glycosidic bonds. The atoms within cellulose crystals are arranged relatively tightly, which renders them impermeable to enzymes and water molecules [13]. It is reported that the oxidation products of cellulose may constitute the core of humic substances under an electric field [14]. For the purpose for recycle agricultural wastes efferently, it should more fundamentally understand the degradation of cellulose in EAB process.

In this study, a series of experiments on cellulose degradation were conducted in electric field. The principal goals of this study were to examine the changes in the physico-chemical properties of degraded cellulose in the presence and absence of an electric field and to illustrate the impact of the electric field on the microbial physiological state. This study provides valuable insights and a deeper understanding of cellulose degradation in EAB process.

2. Materials and methods

2.1. Reagents

The chemical reagents used in this study were analytically pure. *Bacillus subtilis* fermentation powder (bio-67659)

was obtained from Beijing Baiou Bowei Bio-Tech Co., Ltd., China. The valid viable count of *B. subtilis* in this bacteria agent was ≥ 200 billion/g, and the miscellaneous bacteria rate $\leq 0.001\%$. The kits used for bacterial physiological and biochemical activity assays, including ATP, SOD, and PI, were purchased from Solarbio Life Sciences (Shanghai, China).

2.2. Setup of the EAB reactor and the procedure of cellulose degradation

The EAB reactor consists of a reaction box made of polymethyl methacrylate (6 cm \times 6 cm \times 5 cm), electrodes, and direct-current (DC) power (Fig. 1). During the experiment, the electrodes were first positioned on the inner wall of the reaction chamber. The reaction chamber was then filled with ionic resin to maintain appropriate humidity. Next, the mixture of cellulose and *Bacillus* in a non-woven bag with a pore size of 500 mesh was placed in the ionic resin. Finally, the direct-current electric field was applied by connecting the DH1766A-1 DC power (DAHUA Battery Co., Ltd., Beijing, China). This is an open system in which aerobic degradation occurred and oxygen was provided by air. During the experiment, DI water was regularly sprayed onto the resin to maintain the humidity at 55%–65%. The reaction chamber was kept at a constant temperature at 37°C. After a certain period of degradation, cellulose samples were collected and their degradation efficiency was determined using an F800 Cellulose Tester (Hanon Instruments Co., Ltd., Jinan, China) based on the gravimetric method [15].

In order to confirm the superiority of EAB, control experiments were conducted in the EAB reactor without DC power (denoted CB). Except for electric field, all other operation details of CB was kept the same as those in EAB.

2.3. Methods to quantify and characterize cellulose

The original and degraded cellulose samples were washed with DI water to remove impurities and dried at room temperature. The structure and composition of the cellulose samples were analyzed using Nicolet 380 Fourier

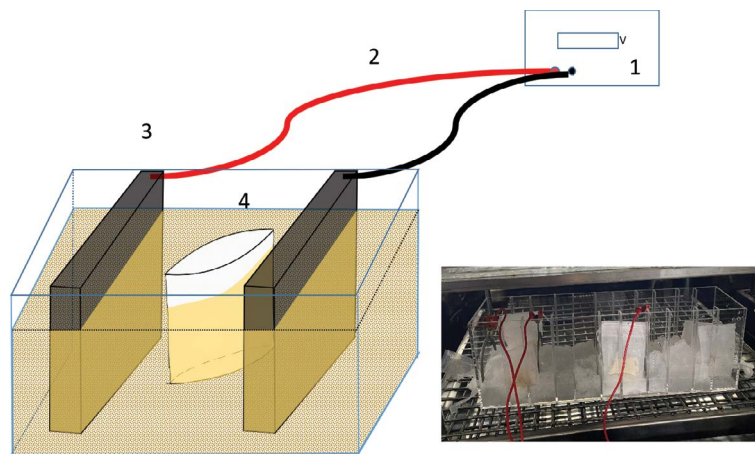


Fig. 1. Schematic diagram of the electric field-assisted biodegradation reactor (1: DC electrical supply; 2: electric wire; 3: electrode; 4: the non-woven bag).

transform infrared spectroscopy (FTIR), with a scanning wavelength range of 400–4,000 cm^{-1} , a resolution of 2 cm^{-1} , and a scanned time of 32. The crystal structure of cellulose was analyzed using Bruker D8 Advance X-ray diffraction (XRD), with a scanning angular (2θ) range of 5°–90° and a scanning speed of 10°/min. The morphology of the cellulose samples was analyzed using ZEISS Sigma 300 scanning electron microscope (SEM), operated at an accelerating voltage of 20 kV. Prior to SEM analysis, the samples were uniformly coated with gold.

2.4. Bacterial physiological and biochemical properties assay methods

To investigate the effects of external electric field on the bacterial physiological and biochemical properties, *B. subtilis* (initial concentration of $\sim 10^6$ CFU/mL) were incubated in Erlenmeyer flasks containing 200 mL TSB at 37°C with various voltage intensities. To monitor the growth of *B. subtilis*, quantification of bacterial cells was performed using the standard plate counting method (CFU/mL) [16]. To analyze cell membrane permeability, flow cytometry (Amnis, Image StreamX Mark II, USA) was used with propidium iodide (PI, Sigma-Aldrich, USA) as a fluorescence indicator [16]. The SOD activity and

cellular ATP levels were determined by using the SOD Assay Kit (Solarbio Life Sciences, Shanghai, China) and Bioluminescence Assay Kit (Solarbio) according to the manufacturer's instructions, respectively [17].

3. Results and discussion

3.1. Degradation of cellulose in EAB

The mass of cellulose in all batches were monitored at specific time intervals, and the degradation rate are shown in Fig. 2. As depicted in Fig. 2a, an initial sharp increase in cellulose degradation rate was observed within the first 24 h. Subsequently, the degradation rate increased slowly after 24 h. At the end of experiments, the degradation rates of cellulose was 9.9% and 17.5% for CB and EAB, respectively. These results suggested that the application of an electric field accelerated the biodegradation of cellulose, which is agreed with the findings of previous reports. Tang et al. reported that, upon applying a direct-current voltage of 2 V, the residual organic matters would decrease from $856 \pm 42 \text{ mg}\cdot\text{L}^{-1}$ to $710 \pm 38 \text{ mg}\cdot\text{L}^{-1}$ [11].

The degradation rate of cellulose increased with the increasing of the electric field intensity (Fig. 1b). In the absence of the low-voltage electric field, the degradation rate of cellulose was only 8.7% after 24 h. Upon application

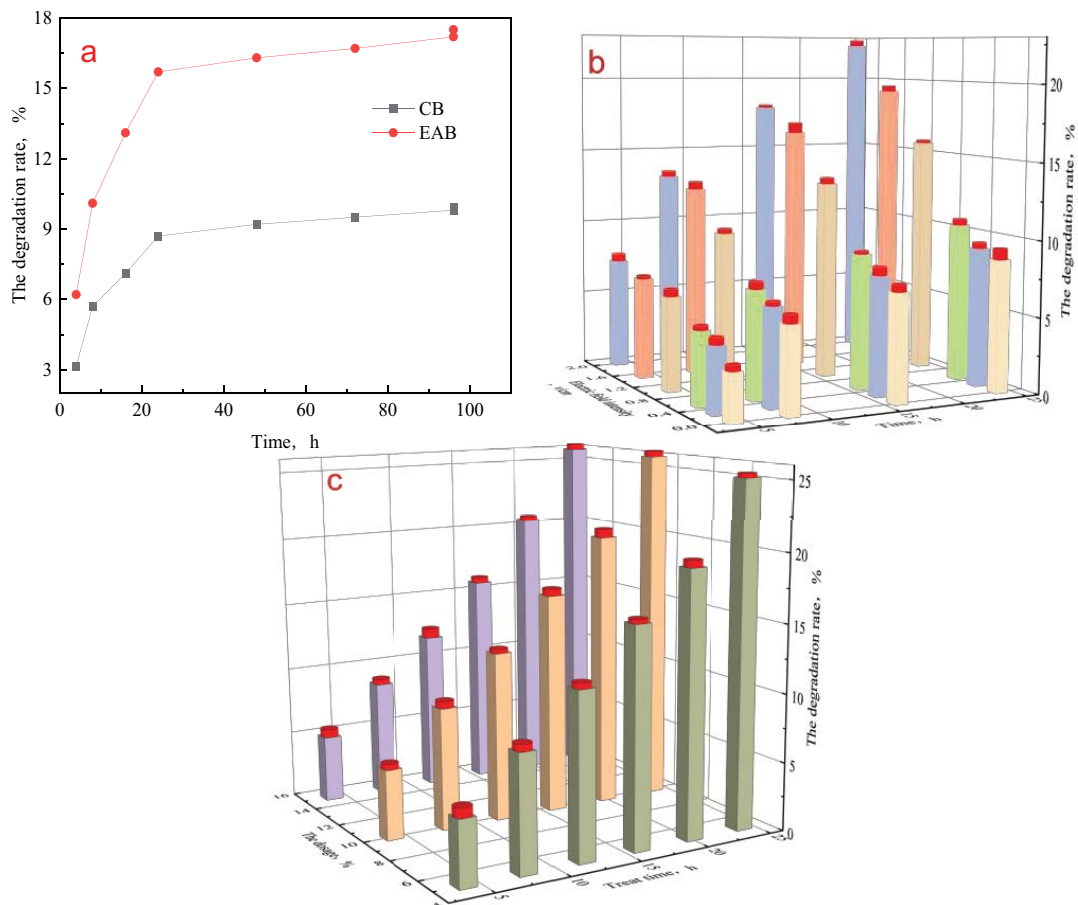


Fig. 2. Degradation rate of cellulose in CB and electric field-assisted biodegradation. (a) the influence of degraded time, (b) the influence of electric field intensity, and (c) the influence of the microbial inoculum dose.

of an electric field intensity less than 0.5 V/cm, the degradation rate of cellulose was mildly increased to 10.4% after 24 h. As the electric field intensity rose to 2 V/cm, the degradation rate of cellulose at 24 h increased to 22.4%, which was 2.57 times of CB.

However, the degradation rate of cellulose was only slightly influenced by the dose of microbial inoculum (Fig. 1c). Specifically, when the initial inoculum dose was 5% and the applied electric field intensity was 2 V/cm, the degradation rate of cellulose at 24 h reached 25.14%. As the initial dose of microbial inoculum was increased to 10% and 15%, the degradation rate of cellulose at 24 h were 25.92% and 25.87%, respectively. In addition, the abundance of microbial species did not affect the overall degradation trend of cellulose. The cellulose degradation rates at different time intervals were similar across all experiments. These findings suggest that once the initial microbial concentration is sufficient for cellulose degradation in EAB, further increasing the microbial concentration has minimal impact on the degradation rate of cellulose.

3.2. Variation of cellulose properties in EAB

Due to their chemical composition and spatial conformation, the cellulose chains tend to form highly organized structural units. The cellulose structure includes crystal regions containing the hydrogen bonding networks and amorphous regions [15]. XRD was used to understand the variation of the crystal and amorphous regions of cellulose as it was degraded in EAB process, and the results are shown in Fig. 3a. The cellulose sample was found to exhibit three significant peaks at 18°, 22.5° and 34.5°. The crystalline structure of cellulose is characterized by the highest

diffraction peak at $2\theta = 22.5^\circ$, while the amorphous structure is indicated by the diffraction peak at $2\theta = 18^\circ$ [18]. Compared to the non-degraded cellulose, the degraded cellulose in CB showed a significant decrease in the intensity of diffraction peaks at 22.5°. This suggests that the crystallinity of cellulose was reduced after the bio-degradation process due to the breaking of hydrogen bonds between cellulose [19]. Moreover, the peak intensity at 22.5° of the degraded cellulose decreased even further as a direct-current voltage of 2 V/cm was applied. This indicated that the electric field would enhance the broken of hydrogen bonds between cellulose. The EAB processes not only reduced the crystallinity but also degraded amorphous cellulose. This was evidenced by the lower intensity of the diffraction peaks at 18° for the degraded cellulose in EAB as compared to the original cellulose. The degradation of both the crystal and amorphous regions of cellulose led to the emergence of new diffraction peaks at $2\theta = 30^\circ$, 40°, 43°, 47°, and 49°, which are attributed to the degradation products of cellulose, including fibrinose and glucose [19]. It should be pointed out that these diffraction peaks of the degraded cellulose products in EAB did not show higher intensities than that in CB. This may be because microbial enzyme could mineralize cellulose directly.

The FTIR analysis is an important support for characterizing the functional groups of cellulose [20]. Fig. 3b illustrates that amorphous cellulose displayed a C–O–C stretching vibration peak of β -glycosidic bond at approximately 890 cm^{-1} on the FTIR spectrum, while a C–O stretching vibration peak appeared at around $1,050\text{ cm}^{-1}$. The absorption peaks at $1,160\text{ cm}^{-1}$ is associated with β -1,4-glycosidic bonds, and the peaks at $1,310$ – $1,370\text{ cm}^{-1}$ represent C=O stretching and C–H bending vibrations. After being degraded in EAB,

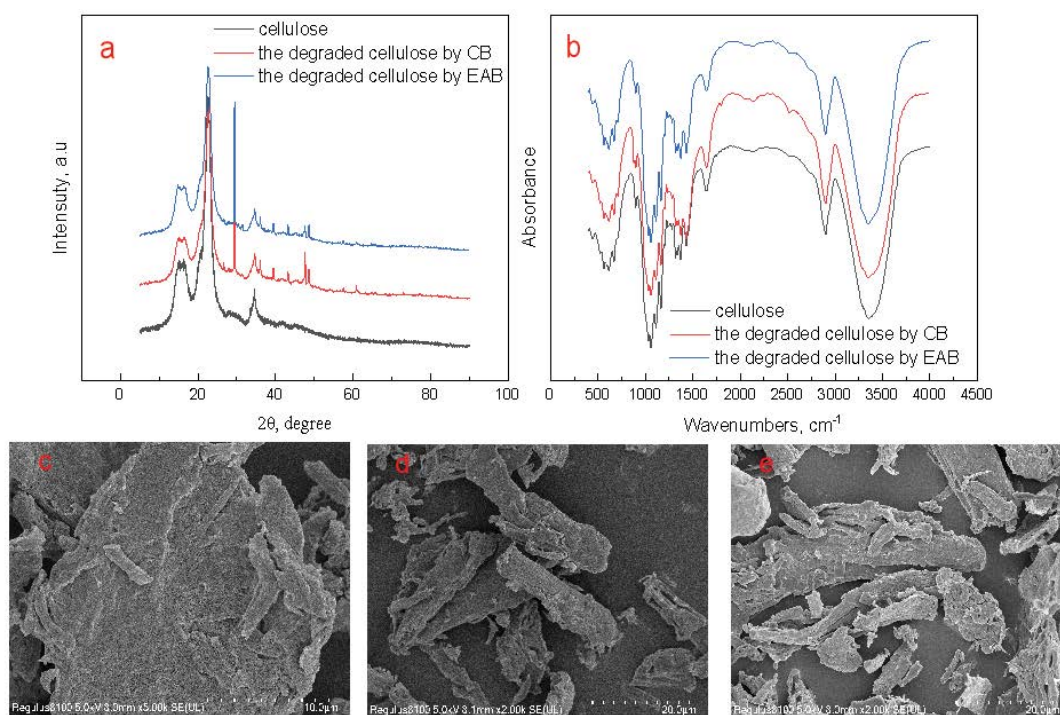


Fig. 3. X-ray diffraction patterns (a), FTIR patterns (b) and SEM images (c–e) of the original and degraded cellulose.

no discernible changes were noted in the FTIR patterns, as depicted in Fig. 3b. The peak location and relative strength of the functional groups of the degraded cellulose were similar with that of the original cellulose. And the C–O–C, C–O, C=O, and C–H groups in cellulose were also present in its degraded products. Therefore, the discernible variation of the functional groups of the cellulose did not be observed after the degradation.

The morphology of cellulose could be affected by the degradation of both crystal and amorphous regions. Fig. 3c clearly shows the width of the cellulose exceeded 15 μm , and its surface was smooth with numerous pores. However, after degradation in CB, the cellulose width decreased significantly, measuring less than 10 μm (Fig. 3d). And some clear wrinkles were observed on the surface of the degraded cellulose in CB. As for the EAB process, the cellulose surface became even rougher, with more wrinkles observed (Fig. 3e). This suggests that compared to CB, EAB causes more serious disruptions for the surface of cellulose.

3.3. Mechanisms of electric field enhanced microbial degradation of cellulose

As aforementioned, EAB showed a higher degradation rates of cellulose than CB. This difference could be attributed to the effect of the low-voltage electric field, which alters the physicochemical properties of cellulose

and enhances the physiological activity of bacteria. To gain a better understanding of the mechanisms involved in electric field enhanced microbial degradation of cellulose, we conducted an analysis of the physicochemical properties of cellulose, as well as the physiological and biochemical properties of *B. subtilis*, under the influence of the low-voltage electric field.

3.3.1. Effects of electric field on the physicochemical properties of cellulose

In the presence of an electric field, oxidation reactions may occur through direct electrolysis in the anode region, as well as indirect electrolysis in the cathode region. To determine whether electrochemical oxidation was responsible for the degradation of the cellulose samples, the degradation rates were measured exclusively under a low-voltage electric field. As shown in Fig. 4a, the degradation rates of cellulose fluctuated in the range of -0.5% – 1.5% at different time interval. Taking the test error into consideration, the quantities of remained largely unchanged with increasing treatment time, suggesting that the level of electrochemical oxidation used in this study was insufficient to degrade cellulose molecular structures.

The XRD patterns of the cellulose treated by the low-voltage electric field displayed three distinct peaks at 18° , 22.5° , and 34.5° , with peak intensities similar to those

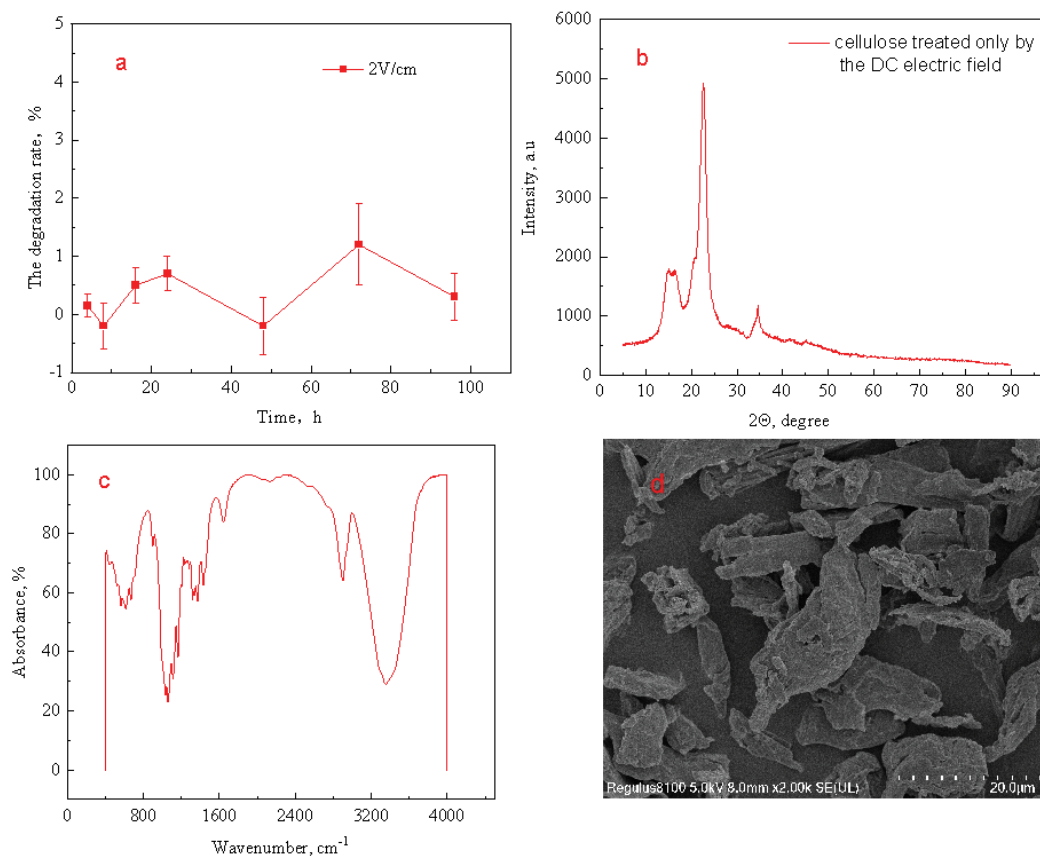


Fig. 4. Degradation rate (a), X-ray diffraction patterns (b), FTIR patterns (c) and SEM images (d) of the cellulose after treated by the low-voltage electric field.

of the original cellulose (Fig. 4b). And no peaks representing degradation products were observed. These results suggested that the crystal and amorphous regions of cellulose did not be degraded by the low-voltage electric field. The FTIR patterns shows that the location and relative strength of C–O–C stretching vibration, C–O stretching vibration, C=O stretching vibration and C–H bending vibration peaks remained unchanged (Fig. 4c). This suggested that the functional groups of the cellulose also did not change after treated by the low-voltage electric field. However, the low-voltage electric field treatment altered the morphology of cellulose. Fig. 4d shows that the previously smooth surface of cellulose became rough, exhibiting several wrinkles. This textured surface facilitates better adherence of microorganisms, leading to an improved degradation rate.

3.3.2. Effects of electric field on physiological and biochemical properties of *B. subtilis*

The underlying principle of electric field enhanced microbial degradation involves inducing changes in the permeability of microbial cell membranes, microbial growth and metabolic activity, microbial community structure, and micro-ecological environment through low voltage application. This process effectively overcomes the energy barrier that hinders the degradation of stubborn organic compounds by microbes [21]. It differs from the mechanism of enhancing direct interspecies electron transfer by adding conductive materials. To gain a deeper understanding of

the mechanism behind the external electric field enhanced microbial degradation of cellulose, we conducted an investigation into its effects on the growth, ATP and SOD activity, and cell membrane permeability of *B. subtilis* (Fig. 5).

Fig. 5a shows the variation of microbial concentration over time in the EAB system at different electric field intensities. The application of an external low voltage was found to enhance the proliferation of *B. subtilis* within the experimental electric field intensity range. Moreover, the increase of electric field intensity promoted the microbial growth rate. The low electric field intensity (0.5 V/cm) insignificantly affected the highest microbial concentration, but instead increased the growth rate of microorganisms. The concentration of *B. subtilis* reached the highest value of $10 \times 10^8/\text{mL}$ after 12 h without electric field, but after 8 h with the presence of low voltage of 0.5 V/cm. When the electric field intensity was further increased to 1 and 2 V/cm, the microbial concentration in the system peaked at $20 \times 10^8/\text{mL}$ after 12 h and 8 h, respectively. Along with the effect of electric field intensity on cellulose degradation efficiency in EAB system (Fig. 1b), it indicates that the external electric field intensity of 1 V/cm or higher enhanced the growth and proliferation rate of *B. subtilis* in the system [22]. This reaction can promote the uptake, utilization, and transformation of cellulose by microorganisms [23], leading to an overall improvement of the degradation efficiency of cellulose. Although the electric field intensity varied, the microbial concentration within the system remained stable between $7\text{--}10 \times 10^8/\text{mL}$ after 24 h.

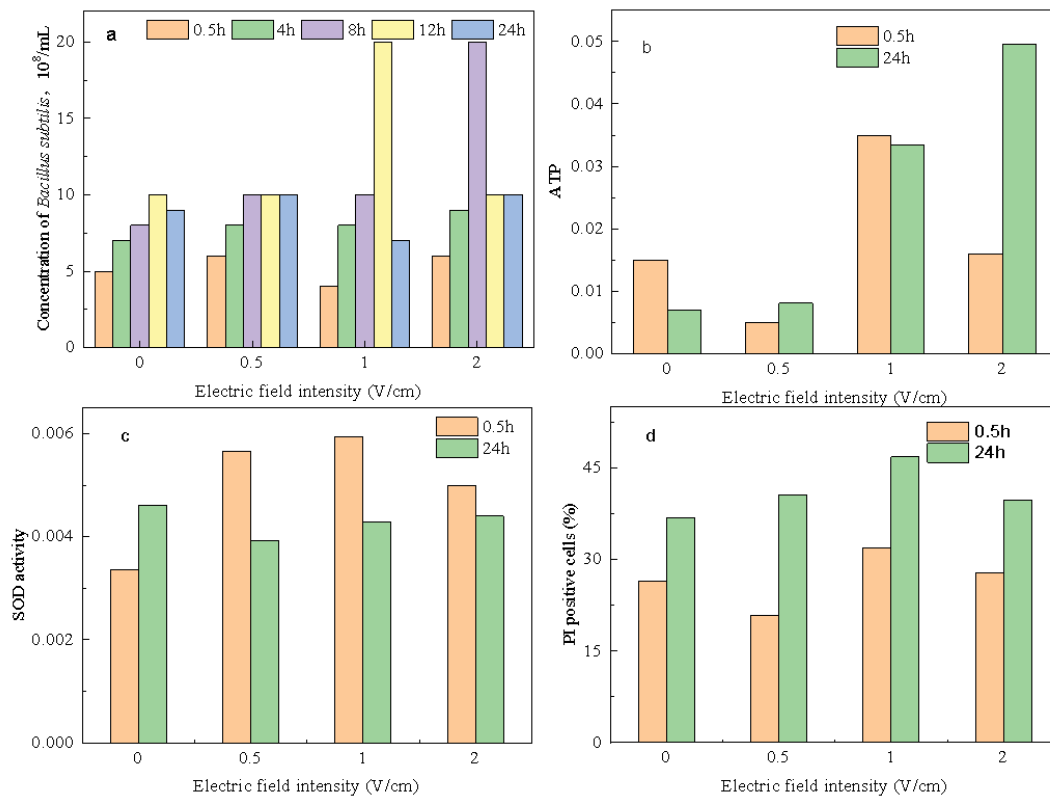


Fig. 5. The growth (a), ATP activity (b), SOD activity (c), and cell membrane permeability (d) of *Bacillus subtilis* in the system with different electric field intensities.

This can be attributed to the consumption of the degradable cellulose within the system. As a result, the remaining cellulose, which was harder to degrade, had to be utilized by the microorganisms present, leading to a sharp decline in bacterial population and decreased proliferation rate.

As shown in Fig. 5b, an increment in the external electric field intensity to 1 and 2 V/cm resulted in a 6-fold increase in microbial ATP activity within the system. This is consistent with the effect of electric field intensity on cellulose degradation efficiency (Fig. 2b) and on the growth of *B. subtilis* (Fig. 5a). The growth of cells is accompanied by the generation of energy substances such as ATP, and the activity of cell ATP enzyme plays an important role in the transport of intracellular and extracellular substances, energy conversion, and information transmission [24,25]. The cell ATP enzyme is essential in maintaining the stability of cell nutrient concentration and is typically utilized to characterize the metabolic activity of cells [24,25]. The high ATP activity indicates a strong ability to degrade organic matter. It demonstrated that the external electric field with intensity of 1 V/cm and higher significantly improved the degradation efficiency of cellulose by increasing microbial metabolic activity.

The bacteria will produce intracellular ROS under adverse external stimulation. If there is excessive accumulation of ROS, it can lead to cell death by oxidation. In response, bacteria would initiate oxidative stress mechanism to increase the activity of reductases to scavenge ROS [26]. SOD is one of the most important reductases, activity generally serves as an indicator of the interference of external stimulation to bacteria. As shown in Fig. 3c, after 0.5 h incubation, *B. subtilis* with low voltage displayed higher SOD activity compared to that without an electric field, with the enzyme activity increasing by 49%–78%. In the range of 0.5–2 V/cm, the SOD activity of *B. subtilis* initially increased and then decreased with increasing electric field intensity. After 24 h of incubation, the SOD activity of *B. subtilis* subjected to low voltage was almost identical to that of the control group without electric field. This suggests that the low intensity external electric field (0.5–2 V/cm) did not cause any significant harmful effects on the physiological and biochemical activity of *B. subtilis* considering the similar bacterial concentration across all experimental conditions. *B. subtilis* could quickly mobilize their oxidative stress system to adapt to the low-voltage electric field and made the intracellular physiological metabolism returned to normal level.

The bacterial cell wall is abundant in charged groups, such as carboxyl, amino, and hydroxyl functional groups, rendering the cell surface negatively charged. This negative charge generates a resting potential of approximately 80 mV across the cell membrane, creating a barrier that restricts the transmembrane transportation of substances [27]. The application of a low-voltage electric field can increase the transmembrane potential, altering the cell membrane permeability and facilitating the uptake of extracellular substances (Fig. 3d). The low-voltage electric field (0.5–2 V/cm) increased the permeability of bacterial cell membrane by 5%–27%. This increase in cell membrane permeability improves the feasibility and efficiency of cellulose transport across the cell membrane, thereby enhancing the cellulose degradation deficiency.

4. Conclusion

This study aimed to investigate the impact of a low-voltage electric field on the degradation of cellulose in EAB through analysis of the physicochemical properties of cellulose and physiological status of microorganisms. The low-voltage electric field caused the surface of cellulose to become rough, resulting in increased adherence of bacteria. Moreover, the microbial ATP activity and membrane permeability increased, indicating higher metabolic activity and improved transport of substances into cells. These effects of the low-voltage electric field contributed to the enhanced degradation of cellulose. At an optimal condition, the cellulose degradation rate in EAB reached 2.57 times that of CB. And the degraded cellulose exhibited a rough and wrinkled surface and reduced crystalline structure. These findings suggest that a low-voltage electric field is a promising approach to enhance cellulose degradation.

Acknowledgment

This work is funded by research fund of China Tobacco Hunan Industrial Co. (KY2022XY0005) and the open fund from the Key Lab of Eco-restoration of Regional Contaminated Environment (Shenyang University), Ministry of Education (Grant no.: KF-22-06), the Laboratory construction and management research project of Shandong University (sy20223601), and the Education and teaching reform research project of Shandong University (2022Y182).

References

- [1] D. Wu, Z. Wei, T.A. Mohamed, G. Zheng, F. Qu, F. Wang, Y. Zhao, C. Song, Lignocellulose biomass bioconversion during composting: mechanism of action of lignocellulase, pretreatment methods and future perspectives, *Chemosphere*, 286 (2022) 131635, doi: 10.1016/j.chemosphere.2021.131635.
- [2] C. Huang, G. Zeng, D. Huang, C. Lai, P. Xu, C. Zhang, M. Cheng, J. Wan, L. Hu, Y. Zhang, Effect of *Phanerochaete chrysosporium* inoculation on bacterial community and metal stabilization in lead-contaminated agricultural waste composting, *Bioresour. Technol.*, 243 (2017) 294–303.
- [3] L. Zhang, J. Zhang, G. Zeng, H. Dong, Y. Chen, C. Huang, Y. Zhu, R. Xu, Y. Cheng, K. Hou, Multivariate relationships between microbial communities and environmental variables during co-composting of sewage sludge and agricultural waste in the presence of PVP-AgNPs, *Bioresour. Technol.*, 261 (2018) 10–18.
- [4] T. Liu, S.K. Awasthi, S. Qin, H. Liu, M.K. Awasthi, Y. Zhou, M. Jiao, A. Pandey, S. Varjani, Z. Zhang, Conversion food waste and sawdust into compost employing black soldier fly larvae (diptera: Stratiomyidae) under the optimized condition, *Chemosphere*, 272 (2021) 129931, doi: 10.1016/j.chemosphere.2021.129931.
- [5] X. Ren, Q. Wang, X. Chen, Y. Zhang, Y. Sun, R. Li, J. Li, Z. Zhang, Elucidating the optimum added dosage of diatomite during co-composting of pig manure and sawdust: carbon dynamics and microbial community, *Sci. Total Environ.*, 777 (2021) 146058, doi: 10.1016/j.scitotenv.2021.146058.
- [6] K. Watanabe, Recent developments in microbial fuel cell technologies for sustainable bioenergy, *J. Biosci. Bioeng.*, 106 (2008) 528–536.
- [7] T. Fu, H. Shangguan, J. Wu, J. Tang, H. Yuan, S. Zhou, Insight into the synergistic effects of conductive biochar for accelerating maturation during electric field-assisted aerobic composting, *Bioresour. Technol.*, 337 (2021) 125359, doi: 10.1016/j.biortech.2021.125359.

- [8] S. Wu, H. He, X. Inthapanya, C. Yang, L. Lu, G. Zeng, Z. Han, Role of biochar on composting of organic wastes and remediation of contaminated soils—a review, *Environ. Sci. Pollut. Res.*, 24 (2017) 16560–16577.
- [9] Y. Liu, X. Li, S. Wu, Z. Tan, C. Yang, Enhancing anaerobic digestion process with addition of conductive materials, *Chemosphere*, 278 (2021) 130449, doi: 10.1016/j.chemosphere.2021.130449.
- [10] Q. Zhou, X. Li, S. Wu, Y. Zhong, C. Yang, Enhanced strategies for antibiotic removal from swine wastewater in anaerobic digestion, *Trends Biotechnol.*, 39 (2021) 8–11.
- [11] J. Tang, X. Li, W. Zhao, Y. Wang, P. Cui, R.J. Zeng, L. Yu, S. Zhou, Electric field induces electron flow to simultaneously enhance the maturity of aerobic composting and mitigate greenhouse gas emissions, *Bioresour. Technol.*, 279 (2019) 234–242.
- [12] J. Wu, Y. Zhao, H. Yu, D. Wei, T. Yang, Z. Wei, Q. Lu, X. Zhang, Effects of aeration rates on the structural changes in humic substance during co-composting of digestates and chicken manure, *Sci. Total Environ.*, 658 (2019) 510–520.
- [13] Y. Wei, D. Wu, D. Wei, Y. Zhao, J. Wu, X. Xie, R. Zhang, Z. Wei, Improved lignocellulose-degrading performance during straw composting from diverse sources with actinomycetes inoculation by regulating the key enzyme activities, *Bioresour. Technol.*, 271 (2019) 66–74.
- [14] Y. Cao, X. Wang, X. Zhang, T. Misselbrook, Z. Bai, L. Ma, An electric field immobilizes heavy metals through promoting combination with humic substances during composting, *Bioresour. Technol.*, 330 (2021) 124996, doi: 10.1016/j.biortech.2021.124996.
- [15] T. Liitiä, S.L. Maunu, B. Hortling, T. Tamminen, O. Pekkala, A. Varhimo, Cellulose crystallinity and ordering of hemicelluloses in pine and birch pulps as revealed by solid-state NMR spectroscopic methods, *Cellulose*, 10 (2003) 307–316.
- [16] Y. Hong, W. Shi, H. Wang, D. Ma, Y. Ren, Y. Wang, Q. Li, B. Gao, Mechanisms of *Escherichia coli* inactivation during solar-driven photothermal disinfection, *Environ. Sci.: Nano*, 9 (2022) 1000–1010.
- [17] H. Xu, Y. Zhu, M. Du, Y. Wang, S. Ju, R. Ma, Z. Jiao, Subcellular mechanism of microbial inactivation during water disinfection by cold atmospheric-pressure plasma, *Water Res.*, 188 (2021) 116513, doi: 10.1016/j.watres.2020.116513.
- [18] T. Ansari, G. Chandra, P. Gupta, G. Joshi, V. Rana, Synthesis of pine needle cyanoethyl cellulose using Taguchi L25 orthogonal array, *Ind. Crops Prod.*, 191 (2023) 115973, doi: 10.1016/j.indcrop.2022.115973.
- [19] H. Zhao, J.H. Kwak, Z.C. Zhang, H.M. Brown, B.W. Arey, J.E. Holladay, Studying cellulose fiber structure by SEM, XRD, NMR and acid hydrolysis, *Carbohydr. Polym.*, 68 (2007) 235–241.
- [20] X. Guo, Y. Wu, IN SITU visualization of water adsorption in cellulose nanofiber film with micrometer spatial resolution using micro-FTIR imaging, *J. Wood Chem. Technol.*, 38 (2018) 361–370.
- [21] X. Zheng, J. Tang, N. Lai, Influence of electric field strength on the microbial degradation of petroleum hydrocarbons, *J. Chem. Technol. Biotechnol.*, 96 (2021) 1573–1579.
- [22] S.-H. Kim, H.-Y. Han, Y.-J. Lee, C.W. Kim, J.-W. Yang, Effect of electrokinetic remediation on indigenous microbial activity and community within diesel contaminated soil, *Sci. Total Environ.*, 408 (2010) 3162–3168.
- [23] M. Hakoda, Y. Hirota, Correlation between dielectric property by dielectrophoretic levitation and growth activity of cells exposed to electric field, *Bioprocess. Biosyst. Eng.*, 36 (2013) 1219–1227.
- [24] S. Dehghani, A. Rezaee, S. Hosseinkhani, Effect of alternating electrical current on denitrifying bacteria in a microbial electrochemical system: biofilm viability and ATP assessment, *Environ. Sci. Pollut. Res.*, 25 (2018) 33591–33598.
- [25] H. Feng, X. Zhang, K. Guo, E. Vaiopoulou, D. Shen, Y. Long, J. Yin, M. Wang, Electrical stimulation improves microbial salinity resistance and organofluorine removal in bioelectrochemical systems, *Appl. Environ. Microbiol.*, 81 (2015) 3737–3744.
- [26] G. Lear, M.J. Harbottle, C.J. van der Gast, S.A. Jackman, C.J. Knowles, G. Sills, I.P. Thompson, The effect of electrokinetics on soil microbial communities, *Soil Biol. Biochem.*, 36 (2004) 1751–1760.
- [27] G. Beretta, A.F. Mastorgio, L. Pedrali, S. Saponaro, E. Sezenna, The effects of electric, magnetic and electromagnetic fields on microorganisms in the perspective of bioremediation, *Rev. Environ. Sci. Bio/Technol.*, 18 (2019) 29–75.